Effects of camera calibration on the accuracy of Unmanned Aerial Vehicle sensor products

Dianah Rose Abeho *1 , **Moreblessings Shoko** 1 , **Patroba Achola Odera** 1

1 University of Cape Town, Division of Geomatics, School of Architecture, Planning and Geomatics, South Africa, abhdia001@myuct.ac.za, m.shoko@uct.ac.za, patroba.odera@uct.ac.za

Abstract

The utilisation of Unmanned Aerial Vehicles (UAV) mounted with non-metric consumer-grade digital cameras is on the rise globally due to their affordability and ease of operation. For high-accuracy UAV products, accurate camera parameters must be determined through camera calibration. Camera calibration can be performed before (pre-calibration) or during the bundle block adjustment (self-calibration). This study aims to analyse the effect of camera calibration parameters on the accuracy of UAV products, namely the Digital Elevation Model (DEM) and orthoimage. Camera calibration parameters are estimated using self-calibration, which deploys 3D image information of the scene in a bundle adjustment, and a 2D reference object-based approach known as Zhang's technique, which requires image information of a planar pattern. This study deployed a DJI FC220 camera mounted on a DJI Mavic Pro UAV. Self-calibration was deployed in Agisoft Metashape software based on Brown's method, and Zhang's technique was deployed in MATLAB and OpenCV. Based on internal accuracy measures, OpenCV yields a minor reprojection error of 0.14, followed by MATLAB (0.79) and self-calibration (1.21). Processing without calibration yields the highest reprojection error of 2.18. Based on external measures of accuracy, that is, the geometric accuracy of UAV products, self-calibration yields the least RMSE of 8.2 and 1.4 cm for the horizontal and vertical, respectively, followed by Zhang's technique with 9.6 and 2.3 cm in MATLAB and 13.5 and 4.3 cm in OpenCV. Processing without calibration yields the highest vertical RMSE of 20.0 and 22.9 cm for the horizontal and vertical, respectively. Comparison of the accuracy of UAV mapping products computed with and without calibration emphasises the need for camera calibration to optimise the accuracy of UAV products. This study recommends assessing other photogrammetric mapping software and camera calibration approaches and the effect of flying heights on calibration parameters and mapping accuracy.

1. Introduction

Unmanned Aerial Vehicle (UAV) technology has become a commonly used tool for data acquisition in geospatial applications due to its ability to produce high spatial resolution images which facilitate the production of high-accuracy photogrammetric products such as maps, orthoimages, 3D models, Digital Elevation Models (DEMs) and point cloud [1-5]. In addition, UAV technology provides a low-cost and flexible alternative to other remote sensing platforms, such as classical aerial photogrammetry and satellite platforms [1, 6, 7]. UAVs are small in size, have autonomous vertical take-off and landing characteristics, have low site requirements, and have high flight safety performance [8]. The utilisation of

UAVs mounted with modern non-metric consumer-grade digital cameras is rising globally due to their affordability and ease of operation [8-10]. A camera consists of an image plane and a lens, which provide a transformation between object space and image space [11]. This transformation is affected by the characteristics of the camera. The commonly used non-metric consumer-grade cameras are characterised by adjustable camera parameters such as principal distance and principal point, and their lenses have relatively large distortions compared to metric and survey-grade cameras [1, 5, 9]. Low-quality lenses in non-metric cameras cause inconsistencies in the camera system, leading to systematic errors that impact UAV product quality [9]. Other aspects that influence the accuracy of UAV-derived

products include the flight parameters (flight height, direction, speed, and image overlaps) and Ground Control Points (GCPs) geometry [12]. Whereas the user has flexibility over the flight parameters used during flight planning, limited UAV/camera options may be available. Optimising the user's available UAV/camera system is essential to achieving optimal accuracy. Applying precise camera calibration parameters for photogrammetric processing with non-metric cameras can help achieve this [13, 14]. Accurate camera parameters and lens distortions compensate for systematic errors in transforming points from object to image space, ensuring quality photogrammetric products [5, 8, 15].

A camera is calibrated if its interior (intrinsic) and exterior (extrinsic) orientation parameters are accurately determined [13, 16]. Intrinsic parameters deal with the camera's internal characteristics, such as focal length, lens distortion (radial and tangential) and coordinates of the image centre [9, 17, 18]. Radial distortion occurs as the curvature of the lens moves away from the centre of the lens. In contrast, tangential distortion is a distortion that occurs when the camera lens and image sensor are not levelled in the manufacturing process [1]. Extrinsic parameters describe the position and orientation of the camera in the space [16, 19]. With the advancements in UAV technology, airborne Global Navigation Satellite Systems (GNSS) and Inertial Navigation System (INS) sensors can accurately determine the location and orientation of the camera in space during a mission [19]. This leaves the question of intrinsic parameters to be addressed since it is essential for scene reconstruction [13, 20] and lens distortion removal, which may translate to a vertical 'doming' of a DEM surface in photogrammetric image processing [5, 8, 21]. It is impossible to overlook how the intrinsic characteristics affect the reconstruction in object space [22].

Camera calibration accuracy has two distinct parts: internal and external accuracy [23]. Internal accuracy concerns the accuracy of recovery of the individual parameters of the calibration model. External accuracy relates to the impact of accuracy on any subsequent photogrammetric measurement derived using camera products, i.e., the effect of calibration errors on object point determination [20]. Internal precision measures include statistical measures such as reprojection errors or estimates of precision such as standard deviation of the estimated parameters. These measures are internal to the triangulation or bundle adjustment process [23] and do not tell us about the precision in object space. Close-range photogrammetry (CRP) focuses on the accuracy of photogrammetric products such as object coordinates [24]. External accuracy assessment can be done by comparing derived object coordinates with the known coordinates whose accuracy exceeds the potential accuracy of the photogrammetric system [23]. Determining coordinates of ground control points (GCPs) can be done by traditional positioning techniques such as traversing or static or Real Time Kinematic (RTK) GNSS observations. In the recent past, smart GCPs, also called aeropoints, have been deployed to collect GNSS data and post-process to resolve coordinates of the control points.

Camera calibration techniques are classified into two broad categories: photogrammetric (3D reference object-based) and self-calibration, with a third in-between category using 2D metric information [25]. 3D reference object-based calibration is performed by observing a calibration object whose geometry in 3D space is known, while self-calibration techniques do not use any calibration object but image information of a static scene [13]. Brown's self-calibration model is a widely used and accepted model in CRP due to its efficiency [17]. The 2D reference object-based method requires the camera to observe a planar pattern shown at different orientations, and one such approach is Zhang's technique, which is considered flexible and robust compared to classical techniques [13, 26]. The most popular camera calibration approach deployed in photogrammetry and Computer Vision (CV) is the self-calibrating bundle adjustment, which was first introduced in the early 1970s by Duane C. Brown [17, 24, 27]. Camera calibration using bundle adjustment is an integral and routinely applied operation within photogrammetric triangulation, especially in high-accuracy close-range measurements [15]. However, with the rapid growth in the adoption of off-the-shelf consumer-grade digital cameras for 3D measurement applications, there are many situations where the geometry of the image network will not support the robust recovery of camera parameters via self-calibration [15, 23]. For this reason, standalone camera calibration remains a requirement and an essential issue in CRP and CV. There is a need to calibrate non-metric cameras both pre-mission and post-mission to cater for variations in the camera parameters caused by camera bumps or vibrations and environments such as temperature, humidity and atmospheric pressure [5, 28].

Different calibration techniques, including laboratory calibration, field calibration, in-situ calibration, self-calibration and open-source CV calibration, have been employed in photogrammetry [15, 17, 19, 23, 28-30]. Laboratory calibration is generally used for metric cameras. The intrinsic parameters are determined in the laboratory using special equipment, so consumer-grade cameras hardly perform laboratory calibration [19]. Field calibration uses terrestrial features that have been precisely surveyed to calibrate camera lenses. This can be achieved conveniently using traditional positioning or GNSS methods [5]. The advantages of field methods are in the accuracy of these points, which have typically been surveyed previously, and the fact that the camera can be used in conditions where it will operate. In-situ or on-the-job calibration indicates a field calibration with the combination of actual object measurements [19]. Calibration parameters are processed by the self-calibrating bundle adjustment technique with Ground Control Points (GCPs) involved.

Similarly, Self-calibration deploys a bundle adjustment technique but doesn't require any known reference points. OpenCV library has become a prevalent tool for camera calibration in CV [23]. The calibration models for CV have traditionally employed reference

grids; the calibration matrix is determined using images of a known object array, such as a checkerboard pattern imaged at different orientations from the camera [15]. The commonly adopted methods include Tsai [31], Heikkila and Silvén [32], Lenz [33] and Zhang [25].

Existing studies have investigated various approaches to computing camera orientation parameters and their accuracies; we present a few examples below. A study by Duran and Atik [24] examined the effect of camera IO parameters obtained from different software on the accuracy of 3D models. Software used included MATLAB, Agisoft lens, Photomodeler and 3D Flow Zephyr. A terrestrial camera (Nikon D800) of 24 mm focal length was used to manually capture images at 50 cm. A 3D model was created using Agisoft photoscan. For the 3D model, the highest and lowest accuracy in planimetry and altimeter were 0.077 m and 0.909 m, respectively, obtained by Agisoft Lens and MATLAB software. Another study by Lim, Seo [1] investigated the impact of camera calibration on the accuracy of DEMs from low percentage overlapping images using an FC300X RBG camera onboard a DJI Phantom 3 UAV. The horizontal and vertical accuracy achieved was 0.003 m and 0.089 m, respectively. Pérez, Agüera [34] investigated the effect of camera calibration on different working conditions, namely laboratory and field. Md4-200 UAV equipped with a non-metric Pentax Optio camera was used at a flight height of 50 m, and Photomodeler scanner software was used for calibration. Field calibration yielded the best results with a reprojection error of 0.282 pix against the laboratory calibration with 1.940 pix. Kršák, Blišťan [35] used low-cost photogrammetry to analyse the accuracy of DEM using a DJI Phantom 2 vision+ UAV at a flight height of 35 m. 5 GCPs were used to validate the DEM by comparing the heights from both methods; a RMSE of 0.048 m was achieved. Different calibration approaches yield different results and accuracies, however there exists limited knowledge on the effect and sensitivity of the computed calibration parameters on the accuracies of photogrammetric products such as orthoimages and DEMs.

This study investigates the impact of intrinsic parameters on the accuracy of the resulting UAV photogrammetric products (orthoimage and DEM. Various approaches and software platforms were used to compute the intrinsic parameters of a DJI FC220 camera. The techniques used include Zhang's 2D reference object-based approach, deployed in OpenCV and MATLAB software and Brown's self-calibration approach, deployed in Agisoft Metashape Professional (MP) software. Calibration parameters derived from these approaches were deployed for processing orthoimages, and the DEM of the study area and the derived products' accuracies were compared.

2. Method

2.1. Study area

The study site is in southwest Uganda in Kabale district, Kitumba sub-county, Omwirwaniro village, see Figure 1. A 30m resolution DEM (Figure 2) extracted from the global Shuttle Radar Topography Mission (SRTM) 1 Arc-Second DEM was used to calculate the slope (Figure 3) across the study area. Slope classes were assigned as follows: gentle ($0 - 15^0$), steep ($16 - 35^0$) and very steep ($36 - 90^0$). It is shown in Figure 2 and 3 that the terrain in the study area is generally steep, with elevation ranging from 1819 to 2160 m above mean sea level. The study area selection was based on the diverse representation of elevation and slope since the study evaluates the effect of camera calibration parameters on the accuracy of the DEM.
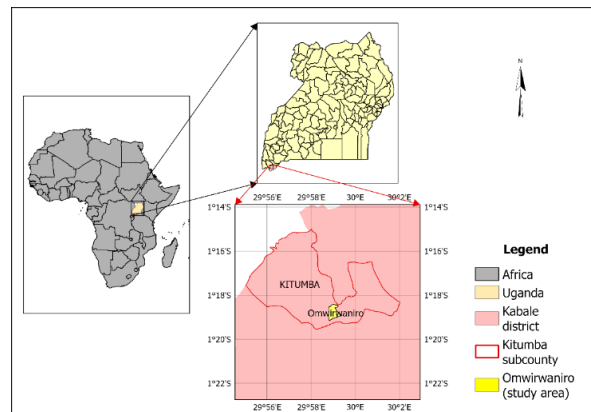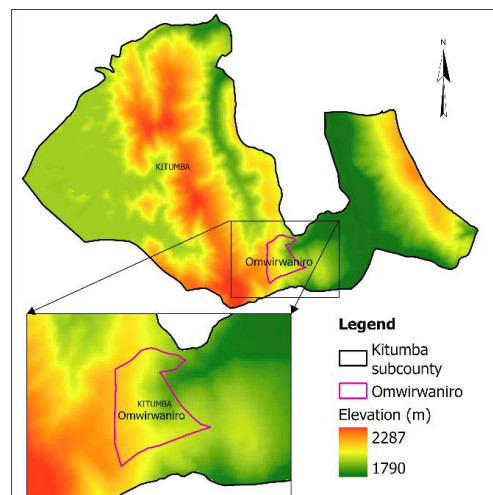

Figure 1. Study area

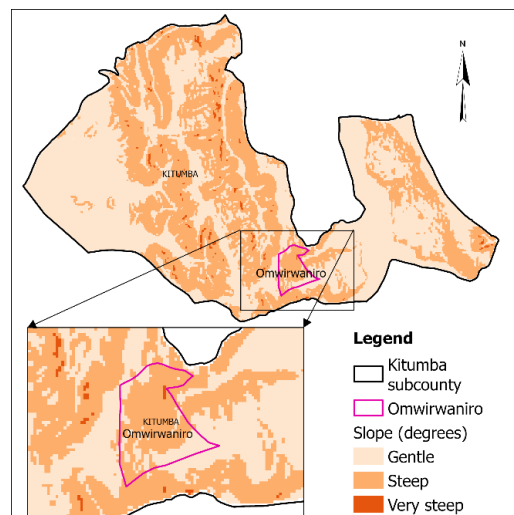**Figure 2.** DEM, Source: (SRTM 1 arc-second DEM)

Figure 3. Slope map

2.2. UAV imaging system

A DJI Mavic Pro UAV and DJI FC220 camera were used for the study (see Figure 4). The Mavic Pro UAV's small size, low weight and foldable design make it easier to operate and store, but they also restrict how well it can endure and perform in windy environments. With DJI's transmission technology, the Mavic Pro UAV can reach up to 7 km in open areas. The Mavic Pro can fly for up to 27 minutes, which may or may not be sufficient for the project's needs and may require more than one battery for longer flights. A 12-megapixel camera with a 3-axis gimbal comes with the Mavic Pro UAV. Detailed specifications of the aircraft and camera/sensor are given in Table 1 and 2, respectively.

Figure 4. DJI Mavic 2 Pro UAV

Table 1. UAV system specifications

Aircraft	DJI Mavic Pro
Folded size	H83mm x W83mm x L198mm
Diagonal Size	335 mm
Weight (Battery & Propellers Included)	743 g (including gimbal cover)
Max Ascent Speed	5 m/s
Max Descent Speed	3 m/s
Max Speed	40 mph in Sport mode without wind
Maximum Take-off Altitude	5000 m
Max Flight Time	27 minutes
Max Hovering Time	24 minutes
Overall, Flight Time	21 minutes
Max Travel Distance	13 km, no wind
Operating Temperature	32° to 104° F (0° to 40° C)
Satellite Positioning Systems	GPS / GLONASS
Hover Accuracy Range	Vertical: +/- 0.1 m to +/-0.5 m
	Horizontal: +/- 0.3 m to +/-1.5 m

Table 2. Camera/sensor specifications

Sensor	(CMOS), 1/2.3"
	Effective pixels:12.35 MP
Camera	DJI FC220
Lens	FOV 78.8° 26 mm
	(35 mm format equivalent) f/2.2
	Distortion < 1.5% Focus from 0.5 m to ∞
ISO Range	photo: 100-1600
Electronic Shutter Speed	8s -1/8000 s
Image Size	4000×3000
Supported Photo format	JPEG, DNG
Operating Temperature	32° to 104° F (0° to 40° C)

2.3. Image acquisition

This study acquired two image data sets: a 2D reference object-based dataset for Zhang's approach and images of the scene for self-calibration. The 2D reference object-based dataset consisted of images of a

checkerboard (Figure 5) used for pre-calibration. The second dataset consisted of images of the scene. The second dataset was also used to map the study site. The datasets are described in detail below.

Data for pre-calibration consisted of images of a 9 by 6, 80 mm square size checkerboard calibration pattern printed on A1 paper captured in manual mode in the field with a DJI FC220 camera mounted on a DJI Mavic Pro UAV. Sixty images of the calibration pattern were taken, and forty-nine images for the calibration exercise were selected. The images were captured with a fixed focus at a distance from the camera, and the calibration pattern covered at least 20% of the image. The images of the calibration pattern were captured at different orientations to the camera (Figure 5). Various images of the pattern were captured to account for the image frame. Including areas near the edges of the pattern ensures accurate estimation of lens distortion, which increases radially away from the centre of the image.
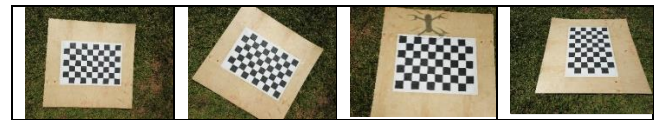

Figure 5. Sample checkerboard images

Data for self-calibration consisted of 280 images of the study area, which were acquired on 17th September 2022 at noon using a DJI FC220 camera mounted on a DJI Mavic Pro UAV. The images were acquired in autonomous flight mode at a flying height of 140 m with 75% front overlap and 65% side lap. Figure 6 shows the UAV flight path defined by camera exposure stations and the distribution of control points and checkpoints. The GCP network constituted 7 GCPs and 3 Check Points (CPs). Coordinates of GCPs and CPs were obtained prior, using triple frequency GNSS receiver (Trimble R8s) in conventional RTK mode. The coordinates of GCPs deployed for RTK bases were determined using 3–5 hours of static GNSS observations with horizontal and vertical accuracy of 1 and 3 cm, respectively. These GCPs were used to validate the 3D and 2D models. During photogrammetric processing, images outside the ground control network were excluded.
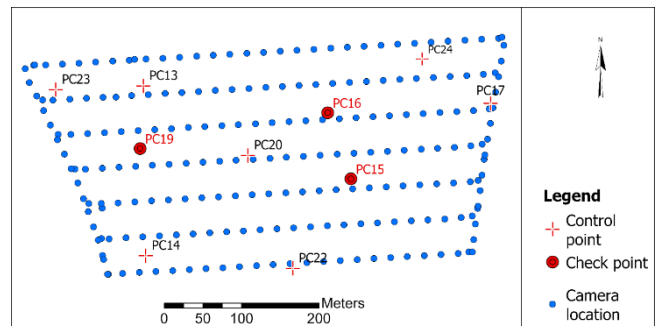

Figure 6. UAV flight path and GCPs

2.4. Estimation of camera parameters

Camera calibration involves determining the relationship between a 3D point in space (X_w, Y_w, Z_w), and its image projection (x, y) [13], represented by Equation 1 [25].

$$\begin{bmatrix} x \\ y \\ 1 \end{bmatrix} = \begin{bmatrix} f_x & 0 & c_x \\ 0 & f_y & c_y \\ 0 & 0 & 1 \end{bmatrix} \begin{bmatrix} r_{11} & r_{12} & r_{13} & t_1 \\ r_{21} & r_{22} & r_{23} & t_2 \\ r_{31} & r_{32} & r_{33} & t_3 \end{bmatrix} \begin{bmatrix} X_w \\ Y_w \\ Z_w \\ 1 \end{bmatrix} \quad (1)$$

f_x, f_y represent the focal length in x and y direction respectively, c_x, c_y, principal point coordinates $[r_{ij}t_i]$, the rotation matrix and translation vector, respectively, are also called extrinsic parameters.

Extrinsic parameters define the position and orientation of the camera in space. The radial (k_1, k_2, k_3) and tangential $(p_1, p_{2)}$ distortions are modelled by Equations 2 and 3 [36].

$$x = x_d + x(k_1 r^2 + k_2 r^4 + k_3 r^8) \\ + [p_1(r^2 + 2x^2) + 2p_2 xy] \quad (2)$$

$$y = y_d + y(k_1 r^2 + k_2 r^4 + k_3 r^8) + [2p_1 xy \\ + p_2(r^2 + 2y^2)] \quad (3)$$

x_d, y_d represent image point coordinates biased by distortions. $r^2 = (x^2 + y^2)$.

This study deploys two approaches to recover intrinsics from the model equations above. Zhang's model was deployed in MATLAB and OpenCV, while Brown's model was deployed in a bundle adjustment in Agisoft MP. Brown's model [37] is one of the most classical physical self-calibration models deployed for camera calibration [8]. Zhang's calibration method is a flexible technique suited for use without specialised knowledge of 3D geometry or CV [25]. Zhang's method is a flexible technique that uses inexpensive equipment compared to classical techniques, advancing 3D CV from a laboratory environment to real-world use [25].

Zhang's calibration method requires a planar checkerboard grid from which the coordinates of the corner points of at least two images with different shooting angles are extracted [15, 25]. İt lies between photogrammetric calibration and self-calibration. The algorithm uses extracted corner points of the checkerboard pattern to compute a projective transformation between the image points of different images [13]. Afterwards, the camera parameters are recovered using a closed-form solution, while radial distortion terms are retrieved within a linear least squares solution [15, 38]. A final non-linear minimisation of the reprojection error, solved using a Levenberg-Marquardt method, refines all the recovered parameters [15, 39].

Using the bundle adjustment approach, Brown's self-calibration model simultaneously determines the intrinsic and extrinsic camera parameters and target coordinates [29, 40]. Self-calibration doesn't require any calibration object. By moving the camera in a static scene, the rigidity of the scene provides two constraints on the cameras' internal parameters from one camera displacement by using image information [25]. Therefore, if the same camera takes images, correspondences between three images are sufficient to recover both the internal and external parameters [16, 13]. In doing so, the self-calibration algorithms make no

or few assumptions about the particular structure of the scene [41]. Using multiple feature points from the scene images, as opposed to a limited number of discrete object points or predefined targets, is beneficial for self-calibration.

This study estimates the camera parameters using Zhang's and Brown's self-calibration approaches. The parameters assessed include the focal length (f_x, f_y), principal point coordinates (c_x, c_y), 3 radial distortion parameters (k_1, k_2, k_3), 2 tangential distortions (p_1, p_2). The subsections below briefly describe the software platforms used.

2.4.1. OpenCV

Open CV is an open-source computer vision and machine learning software library with various interfaces, including Python, C++, Java, and MATLAB. It supports Windows, Linux, Android, and Mac operating systems. In this study, the Python interface was used to estimate calibration parameters. The Python code used to calculate calibration parameters employs Zhang's calibration method, extracted from https://docs.opencv.org/4.x/dc/dbb/tutorial_py_calibration.html and modified to suit the project data.

2.4.2. MATLAB

The camera calibration tool in MATLAB was used to estimate the camera intrinsic and lens distortion parameters using checkerboard images. The accuracy of estimated camera parameters was evaluated, and modifications (such as eliminating images with poor image qualities) were made to improve the accuracy. MATLAB camera calibration deploys Zhang's calibration method.

2.4.3. Agisoft Metashape Professional

Agisoft Metashape software was used to compute camera calibration parameters. Agisoft Metashape deploys the self-calibration approach (Brown's approach) using the bundle block adjustment to estimate the camera calibration matrix, lens distortion coefficients and target coordinates. Agisoft is among the most common commercial tools used to process UAV data and can handle various data types, including different image file formats, point clouds, and meshes [42].

2.5. Orthoimage and DEM generation

Three sets of camera calibration parameters estimated using the approaches discussed in Section 2.4 are deployed in Agisoft MP for orthoimage and DEM production. The fourth set of parameters was generated assuming a perfect lens without any distortions and that the image coordinate system's geometric centre coincides with the sensor's centre; this category is called "no calibration". Agisoft MP is a robust software package widely used to process digital images and 3D spatial data using the Structure from Motion (SfM) approach.

7 GCPs were used to georeference the images during photogrammetric processing. An accuracy assessment of the photogrammetric products (orthoimage, DEM) was

performed using 3 Check Points (CPs). The horizontal and vertical Root Mean Square Error (RMSE) gives the difference between the 3D UAV photogrammetry and reference (GNSS) coordinates of the CPs using Equations 4 to 7 [2]. The other external accuracy measure is the spatial resolution.

$$RMSE_X = \left\{ \frac{1}{n} \sum_{i=1}^{n} [X_{UAV} - X_{GNSS}]^2 \right\}^{\frac{1}{2}} \qquad (4)$$

$$RMSE_Y = \left\{ \frac{1}{n} \sum_{i=1}^{n} [Y_{UAV} - Y_{GNSS}]^2 \right\}^{\frac{1}{2}} \qquad (5)$$

$$RMSE_Z = \left\{ \frac{1}{n} \sum_{i=1}^{n} [Z_{UAV} - Z_{GNSS}]^2 \right\}^{\frac{1}{2}} \qquad (6)$$

$$RMSE_{XY} = \sqrt{RMSE_X^2 + RMSE_Y^2} \qquad (7)$$

n is the number of compared pairs, $RMSE_X$ is the error in the X direction, $RMSE_Y$ is the error in the Y direction, $RMSE_Z$, is the error in the elevation, and $RMSE_{XY}$, is the horizontal error. The RMSE is calculated independently at each check point and averaged across all check points in the horizontal and vertical directions [2].

3. Results and discussion

3.1. Camera calibration parameters

Camera calibration parameters were estimated using the three software platforms (MATLAB, OpenCV and Agisoft MP). The parameters are tabulated in Table 3. For visualisation and comparison, graphs were prepared (see Figure 7, 8 and 9). For each estimated set of camera calibration parameters, the Reprojected Error (RE) is computed as the internal measure of accuracy. The RE (measured in pixels) defines the distance between the reprojection of a model estimation (points reprojected using camera parameters) and its corresponding true projection (points detected from the image). The closer the reprojection error is to zero, the more accurate the parameters determined are. The MATLAB manual indicates an acceptable mean reprojection error of less than one pixel.

Table 3. Camera calibration parameters

	MATLAB	OpenCV	Agisoft MP	No calibration
F (mm)	4.72	4.72	4.66	4.73
C_x (pix)	1971.50	1967.80	1965.33	0
C_y (pix)	1554.71	1532.43	1536.82	0
k_1	0.35619	0.35951	0.06091	0
k_2	-2.28662	-2.32179	-0.12754	0
k_3	4.49235	4.77628	0.10784	0
p_1	-0.00236	-0.00383	5.06613	0
p_2	-0.00161	-0.00146	0.00011	0
RE (pix)	0.79	0.14	1.21	2.18

Figure 7 demonstrates that the estimated focal length calculated using Zhang's approach in MATLAB and OpenCV is similar and closer to the known (priori) value, with a difference of 0.01 mm. The discrepancy between the focal length estimated using Brown's self-calibration approach and the known value is 0.07 mm.
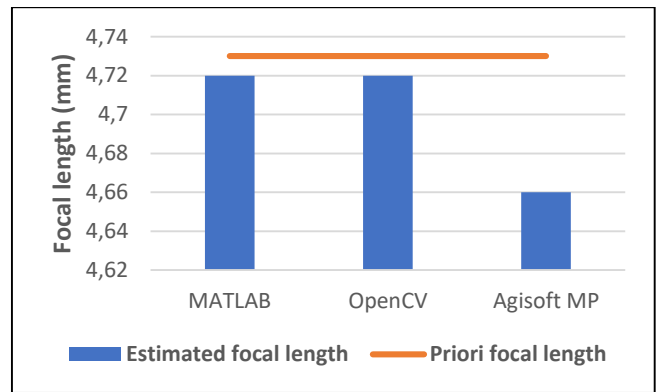

Figure 7. Comparison of estimated and priori focal length

Figure 8 shows the radial distortion parameters (k_1, k_2, k_3), computed using the three approaches. Agisoft MP yieled the smallest tangential distortions, close to zero. The tangential and radial distortions of MATLAB and OpenCV are comparable and higher than those of Agisoft MP, see Figure 8.
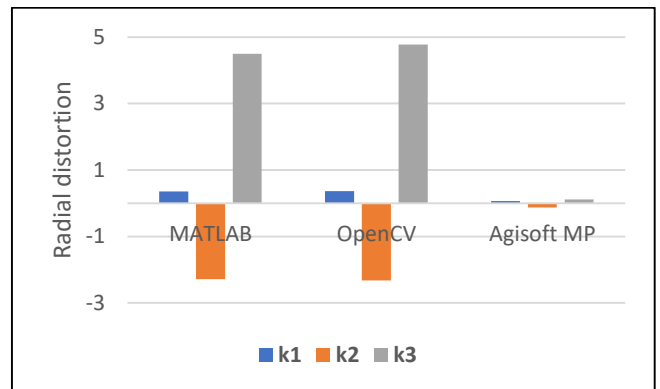

Figure 8. Comparison of radial distortion parameters

As shown in Figure 9, the tangential distortion is near zero for MATLAB and OpenCV, but increases for Agisoft MP. Zhang's calibration approach is used in MATLAB and OpenCV, which may explain why the distortion parameters are comparable yet different from those computed using Brown's approach in Agisoft MP.
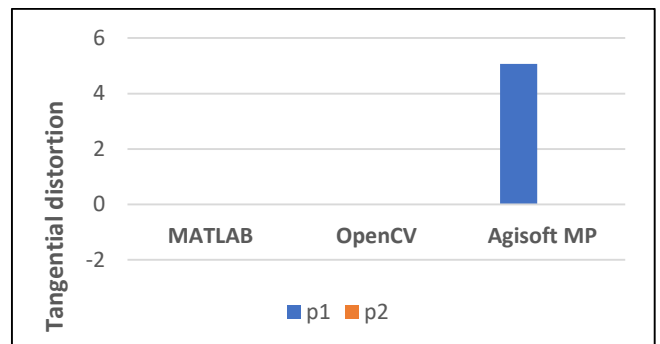

Figure 9. Comparison of tangential distortion parameters

The principal point coordinates vary slightly between the three approaches. Figure 10 shows that OpenCV performs best with a reprojection error of 0.14 pix, followed by MATLAB with 0.79 pix, self-calibration with 1.21 pix and "no calibration" with 2.18 pix.
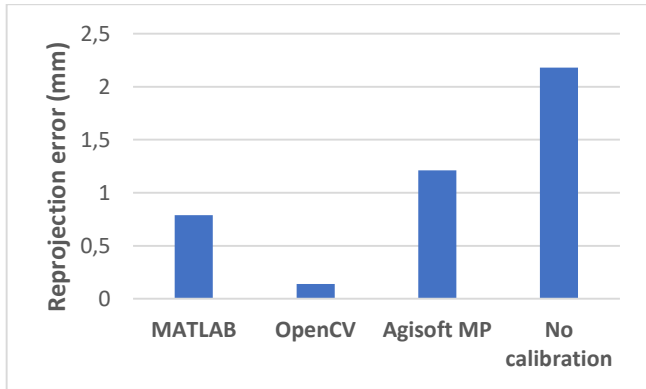
Figure 10. Reprojection error

Other precision measures of the computed parameters for self-calibration in Agisoft MP include standard deviations for each estimated parameter, provided in the covariance matrix produced by bundle adjustment (see Figure 11).

Figure 11. Calibration coefficients and covariance matrix

The covariance matrix (Figure 11) computed during the bundle adjustment in Agisoft MP captures the uncertainty of the object/image transformation. Column 2 represents the adjusted calibration parameters, and column 3 the respective standard deviations. The focal length units are pixels, while the principal point coordinates are offsets from the image centre. Off-diagonal elements are covariances, σ_{ii}, which reflect the degree of correlation between the corresponding parameters. Internal measures of precision focus on the accuracy with which the camera parameters are determined rather than the accuracy of the photogrammetric products derived using these calibration parameters. As a result, additional testing was conducted to assess the impact of the estimated camera calibration parameters on computed photogrammetric products; the findings are presented in Section 3.2.

3.2. Orthoimage and DEM generation

The photogrammetric products generated using the interior orientation parameters provided in Table 3 are shown in Figure 12 and 13. The external accuracy assessment results of the orthoimage and DEM are presented in Table 4. The RMSE represents the difference between the UAV photogrammetry and reference 3D coordinates of the checkpoints. A lower RSME indicates a reduced disparity between the two data sets. The Ground Sample Distance (GSD) represents the spatial resolution of the orthoimage. A lower GSD value signifies higher spatial resolution and more visible details. The DEM resolution denotes the area on the ground being represented by one image pixel; a lower resolution value indicates higher accuracy.

Table 4. Precision measures

	MATLAB	OpenCV	Agisoft MP	No calibration
RMSE xy (m)	0.0964	0.1346	0.0818	0.2004
RMSE z (m)	0.0230	0.0428	0.0142	0.2290
Reprojection error (pix)	0.79	0.14	1.21	2.18
Orthoimage resolution (GSD)(cm/pix)	4.74	4.74	4.72	4.74
DEM resolution (cm/pix)	9.48	9.48	9.69	9.48

The accuracy measure (RMSE) of the photogrammetric products is an external measure of the accuracy of the estimated calibration parameters. Self-calibration (*Agisoft MP)* produces the least horizontal RMSE of 8.2 cm, followed by MATLAB with 9.6 cm, OpenCV with 13.5 cm, and the highest is 20 cm for "No calibration". The vertical RMSE is 1.4 cm for self-calibration, 2.3 cm for MATLAB, 4.3 for OpenCV and 22.9 for "No calibration". Based on RMSE, self-calibration gives the best results, followed by MATLAB and OpenCV. This demonstrates that different calibration techniques impact photogrammetric processing results differently. "No calibration", that is, assuming that the lens and sensor are in perfect condition, yields the highest RMSE. To acquire the best results, the calibration technique should be selected carefully. The results of this study are comparable to the results of existing research conducted by Duran and Atik [24]. Duran's study compared camera calibration results using various photogrammetric software, namely Agisoft Lens, Photomodeler, 3D Flow Zephyr and MATLAB. Data was collected using a Nikon D800 camera. Agisoft Lens was then used to generate a 3D model using the computed interior orientation parameters. The RMSE (3D) was computed at 7 check points as 7.7 cm, 41.2 cm, 45 cm and 90.9 cm for Agisoft Lens, Photomodeler, 3D F Zephyr and MATLAB. The 3D RMSE obtained using interior orientation parameters computed using Agisoft MP and Agisoft Lens are comparable.

The spatial resolution of the orthoimage and DEM is 4.7 cm and 9–10 cm, respectively, suggesting that the deviation in the camera calibration parameters has no significant effect on the spatial resolution (GSD) of the photogrammetric products, but the geometric accuracy (RMSE). In addition to camera focal length, which varies slightly for this study, spatial resolution depends on the flight height and sensor width, which are constant for this study. This may explain the resulting minimal variation in the spatial resolution of the photogrammetric products. We note that various parameters affect the accuracy of photogrammetric products, including front

and side overlaps, GCPs and image processing software. This investigation used the same dataset for photogrammetric processing; therefore, these parameters remained consistent.

Zhang's technique demonstrates higher performance based on the internal accuracy measure (RE), while self-calibration performs better based on the external measures (RMSE) of accuracy. The cause of this discrepancy was not investigated in this study.
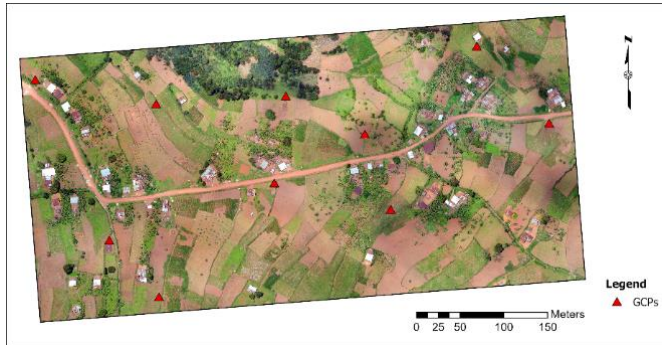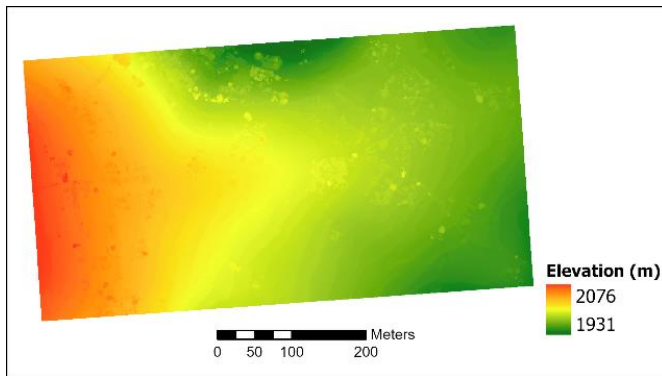

Figure 12. Orthoimage

Figure 13. Digital elevation model

4. Conclusion and recommendation

This study was done to determine the effect of various camera calibration approaches on the accuracy of photogrammetric products, specifically orthophoto and DEM. Two calibration approaches (Zhang's and Brown's) were used to estimate calibration parameters in MATLAB, OpenCV and Agisoft MP software packages. The study's findings show that the calibration approaches and software produced different outcomes. Brown's self-calibration approach, implemented in Agisoft MP, achieved the best horizontal (8.2 cm) and vertical (1.4 cm) RMSE. The results show that camera calibration parameters substantially affect the geometric accuracy of photogrammetric products. Horizontal accuracy improved by 12 cm, and vertical accuracy increased by 22 cm. This means that camera calibration improved the geometric accuracy of the photogrammetric products by 60% horizontally and 96% vertically. The comparison of accuracy between self-calibration and "no calibration" derived camera parameters emphasises the need for camera calibration to optimise the accuracy of derived photogrammetric products. This underscores the importance of camera calibration in executing UAV surveys using non-metric consumer-grade cameras. The results achieved in this study are confined to the DJI FC220 camera and the scope of this study.

The study deployed Zhang's and brown's calibration models to compute calibration parameters and Agisoft MP software to generate the photogrammetric mapping products. It is recommended that various calibration models, photogrammetric software, and other non-metric UAV cameras be examined, as they are routinely used for geospatial data acquisition. Further examination of the mathematical models is necessary to determine the cause of variances in MATLAB and OpenCV's reprojection errors. Brown's self-calibration approach produced a lower RMSE than Zhang's approach, and the vice versa is true for the reprojection error; future research may study the reasons behind this. The influence of varying flying heights on calibration parameters and mapping accuracy was not in the scope of this study, but it may be worth investigating.

Acknowledgement

Author contributions

Dianah Rose Abeho: Conceptualization, Methodology, Field work, Data processing, Validation, Data curation, Writing – Original draft preparation **Moreblessings Shoko:** Conceptualization, Methodology, Writing-Reviewing and Editing **Patroba Achola Odera:** Conceptualization, Methodology, Writing-Reviewing and Editing.

Conflicts of interest

The authors declare no conflicts of interest.

References

1. Lim P, Seo J, Son J, Kim T. Analysis of orientation accuracy of an UAV image according to camera calibration. International Archives of the Photogrammetry, Remote Sensing & Spatial Information Sciences. 2019; XLII-2/W13.
2. Elkhrachy I. Accuracy assessment of low-cost Unmanned Aerial Vehicle (UAV) photogrammetry. Alexandria Engineering Journal. 2021;60(6):5579-90.
3. Zhou Y, Rupnik E, Meynard C, Thom C, Pierrot-Deseilligny M. Simulation and analysis of photogrammetric UAV image blocks—Influence of camera calibration error. Remote sensing. 2019;12(1):22.
4. He F, Zhou T, Xiong W, Hasheminnasab SM, Habib A. Automated aerial triangulation for UAV-based mapping. Remote Sensing. 2018;10(12):1952.
5. Sanz-Ablanedo E, Chandler JH, Ballesteros-Pérez P, Rodríguez-Pérez JR. Reducing systematic dome

errors in digital elevation models through better UAV flight design. Earth Surface Processes and Landforms. 2020;45(9):2134-47.

6. James MR, Robson S. Mitigating systematic error in topographic models derived from UAV and ground-based image networks. Earth Surface Processes and Landforms. 2014;39(10):1413-20.

7. Pathak S, Acharya S, Bk S, Karn G, Thapa U. UAV-based topographical mapping and accuracy assessment of orthophoto using GCP. Mersin Photogrammetry Journal. 2024;6(1):1-8.

8. Huang W, Jiang S, Jiang W. Camera self-calibration with GNSS constrained bundle adjustment for weakly structured long corridor UAV images. Remote Sensing. 2021;13(21):4222.

9. Kılınç Kazar G, Karabörk H, Makineci HB. Evaluation of test field-based calibration and self-calibration models of UAV integrated compact cameras. Journal of the Indian Society of Remote Sensing. 2022;50(1):13-23.

10. Cramer M, Przybilla H-J, Zurhorst A. UAV cameras: Overview and geometric calibration benchmark. The International Archives of the Photogrammetry, Remote Sensing and Spatial Information Sciences. 2017;42:85-92.

11. Dzurisin D, Thompson RA, Schilling SP. Photogrammetry. Volcano Deformation: Geodetic Monitoring Techniques. 2007:195-221.

12. Kozmus Trajkovski K, Grigillo D, Petrovič D. Optimization of UAV flight missions in steep terrain. Remote Sensing. 2020;12(8):1293.

13. Huang W, Peng X, Li L, Li X. Review of Camera Calibration Methods and Their Progress. Laser & Optoelectronics Progress. 2023;60(16):1600001--11.

14. Sharma M, Raghavendra S, Agrawal S. Development of an open-source tool for UAV photogrammetric data processing. Journal of the Indian Society of Remote Sensing. 2021;49(3):659-64.

15. Remondino F, Fraser C. Digital camera calibration methods: considerations and comparisons. International Archives of the Photogrammetry, Remote Sensing and Spatial Information Sciences. 2006;36(5):266-72.

16. Zhang Z. Camera parameters (intrinsic, extrinsic). Computer Vision: A Reference Guide: Springer; 2021. p. 135-40.

17. Tang R. Mathematical methods for camera self-calibration in photogrammetry and computer vision 2013.

18. Guo K, Ye H, Gu J, Chen H. A novel method for intrinsic and extrinsic parameters estimation by solving perspective-three-point problem with known camera position. Applied Sciences. 2021;11(13):6014.

19. Hadi AH, Khalaf AZ. Accuracy Assessment of Establishing 3D Real Scale Model in Close-Range Photogrammetry with Digital Camera. Engineering and Technology Journal. 2022;40(11):1492-509.

20. Roncella R, Forlani G. UAV block geometry design and camera calibration: A simulation study. Sensors. 2021;21(18):6090.

21. Carbonneau PE, Dietrich JT. Cost-effective non-metric photogrammetry from consumer-grade sUAS: implications for direct georeferencing of structure from motion photogrammetry. Earth surface processes and landforms. 2017;42(3):473-86.

22. Hastedt H, Luhmann T. Investigations on the quality of the interior orientation and its impact in object space for UAV photogrammetry. The International Archives of the Photogrammetry, Remote Sensing and Spatial Information Sciences. 2015;40:321-8.

23. Luhmann T, Fraser C, Maas H-G. Sensor modelling and camera calibration for close-range photogrammetry. ISPRS Journal of Photogrammetry and Remote Sensing. 2016;115:37-46.

24. Duran Z, Atik ME. Accuracy comparison of interior orientation parameters from different photogrammetric software and direct linear transformation method. International Journal of Engineering and Geosciences. 2021;6(2):74-80.

25. Zhang Z. A flexible new technique for camera calibration. IEEE Transactions on pattern analysis and machine intelligence. 2000;22(11):1330-4.

26. Li W, Gee T, Friedrich H, Delmas P, editors. A practical comparison between Zhang's and Tsai's calibration approaches. 29th International Conference on Image and Vision Computing 2014 November 2014; New Zealand.

27. Gruen A, Beyer HA. System calibration through self-calibration. Calibration and orientation of cameras in computer vision: Springer; 2001. p. 163-93.

28. Wolf PR, Dewitt BA, Wilkinson BE. Elements of Photogrammetry with Applications in GIS: McGraw-Hill Education; 2014.

29. Clarke TA, Fryer JG. The development of camera calibration methods and models. The Photogrammetric Record. 1998;16(91):51-66.

30. Luhmann T, Robson S, Kyle S, Harley I. Close range photogrammetry: principles, techniques and applications: Whittles publishing Dunbeath; 2006.

31. Tsai RY, editor An efficient and accurate camera calibration technique fro 3d machine vision. CVPR'86; 1986.

32. Heikkila J, Silvén O, editors. A four-step camera calibration procedure with implicit image correction. IEEE computer society conference on computer vision and pattern recognition; 1997 17-19 June 1997; San Juan, PR, USA: IEEE.

33. Lenz R. Lens distortion corrected CCD-camera calibration with co-planar calibration points for real-time 3D measurements. Prodding of ISPRS, Fast Processing of Photogrammetric Data, 1987. 1987:60-7.

34. Pérez M, Agüera F, Carvajal F. Digital camera calibration using images taken from an unmanned aerial vehicle. International archives of the photogrammetry, remote sensing and spatial information sciences. 2011;38(1/C22).

35. Kršák B, Blišťan P, Pauliková A, Puškárová P, Kovanič Ľm, Palková J, et al. Use of low-cost UAV photogrammetry to analyze the accuracy of a digital elevation model in a case study. Measurement. 2016;91:276-87.

36. Drap P, Lefèvre J. An exact formula for calculating inverse radial lens distortions. Sensors. 2016;16(6):807.
37. Brown CD. Close-range camera calibration. Photogramm Eng. 1971;37(8):855-66.
38. Yan L, Tengfei L. Research on the improvement of Zhang Zhengyou's camera calibration method [J]. Optical technology. 2014;40(06):565-70.
39. Prakash CD, Karam LJ, editors. Camera calibration using adaptive segmentation and ellipse fitting for localizing control points. 2012 19th IEEE International Conference on Image Processing; 2012: IEEE.
40. Hemayed EE, editor A survey of camera self-calibration. Proceedings of the IEEE Conference on Advanced Video and Signal Based Surveillance, 2003; 2003: IEEE.
41. Liu S, Peng Y, Sun Z, Wang X. Self-calibration of projective camera based on trajectory basis. Journal of Computational Science. 2019;31:45-53.
42. Kingsland K. Comparative analysis of digital photogrammetry software for cultural heritage. Digital Applications in Archaeology and Cultural Heritage. 2020;18:e00157.